

Condensation of isolated metal clusters studied with a calorimeter

T. Bachels, F. Tiefenbacher, and R. Schäfer

Citation: *The Journal of Chemical Physics* **110**, 10008 (1999); doi: 10.1063/1.478874

View online: <http://dx.doi.org/10.1063/1.478874>

View Table of Contents: <http://scitation.aip.org/content/aip/journal/jcp/110/20?ver=pdfcov>

Published by the [AIP Publishing](#)

Articles you may be interested in

[Examining the heavy p-block with a pseudopotential-based composite method: Atomic and molecular applications of rp-ccCA](#)

J. Chem. Phys. **137**, 214111 (2012); 10.1063/1.4768420

[Guided ion beam studies of the reactions of \$\text{Co}_n + \(n = 1 - 18\)\$ with \$\text{N}_2\$: Cobalt cluster mononitride and dinitride bond energies](#)

J. Chem. Phys. **128**, 194313 (2008); 10.1063/1.2909978

[Metal-carbon clusters: The origin of the delayed atomic ion](#)

J. Chem. Phys. **124**, 164304 (2006); 10.1063/1.2171692

[Atomization enthalpies and enthalpies of formation of the germanium clusters, \$\text{Ge}_5\$, \$\text{Ge}_6\$, \$\text{Ge}_7\$, and \$\text{Ge}_8\$ by Knudsen effusion mass spectrometry](#)

J. Chem. Phys. **112**, 7443 (2000); 10.1063/1.481343

[Kinetics of the condensation of Cs from its supersaturated vapor: Comments on the entropy of a small Cs cluster](#)

J. Chem. Phys. **111**, 8265 (1999); 10.1063/1.480333



Condensation of isolated metal clusters studied with a calorimeter

T. Bachels, F. Tiefenbacher, and R. Schäfer

Institut für Physik, Universität Basel, Klingelbergstrasse 82, CH-4056 Basel, Switzerland

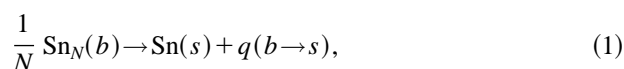
(Received 8 December 1998; accepted 24 February 1999)

We describe the combination of molecular beam techniques with a calorimeter in order to investigate thermal properties of isolated metal clusters. A size distribution of neutral Sn_N clusters with $6 \leq N \leq 600$ is deposited on a bimetallic micromechanical sensor and the released heat during the cluster deposition can be determined from the time-dependent bending of the sensor. The size distribution of the deposited clusters coming from the pulsed source has been probed with a quasicontinuous time-of-flight mass spectrometer. The formation enthalpy per atom of the investigated Sn_N cluster size distribution is obtained from the measured calorimetric heat to $\Delta h_{f,298} = 0.45 - 0.53$ eV. © 1999 American Institute of Physics. [S0021-9606(99)02619-7]

INTRODUCTION

The mass spectrometric investigation of the composition of metal vapors allows the determination of formation and atomization enthalpies of small metal clusters, provided the clusters are present under equilibrium conditions and sufficiently low vapor densities to allow the analysis by means of the ideal gas behavior.¹ This Knudsen mass spectrometric technique has been applied to the examination of metal clusters M_N with up to $N=7$ atoms.² The ideal gas condition breaks down if the vapor density is enhanced in order to shift the equilibrium to higher partial pressures of larger cluster species. Therefore, the Knudsen cell technique can hardly be applied for the thermodynamic investigation of larger clusters with $N>7$. For the exploration of thermal properties of these larger clusters molecular beam techniques provide the possibility to generate large metal clusters M_N with up to $N \approx 1000$ atoms.³ However, one has to notice that the cluster formation in molecular beam experiments is a result of an interplay between thermodynamics and kinetics, i.e., the cluster formation itself is a complicated nonequilibrium process, which prevents a determination of the thermal properties of isolated clusters present in a molecular beam from a mass spectrometric investigation. However, King and co-workers have demonstrated, how it is possible to determine the binding energies of molecules from molecular beam experiments on a solid surface.⁴ Campbell and co-workers have expanded these experiments to the examination of metal atom beams.⁵ Both groups have developed calorimetric techniques, which allow them to measure the released heat during the deposition of the molecular beam onto a solid substrate. In order to obtain, for example, the formation or sublimation enthalpies of the metal atoms present in the atomic beam, they have corrected the calorimetrically measured heats taking the nonequilibrium situation of the metal atom deposition process into account. This correction allows them to determine formation enthalpies of metal atoms, which are equivalent to the data obtained from the investigation of the metal vapor in equilibrium with a solid surface. In order to study the thermal properties of isolated clusters generated in molecular beam experiments we have combined

these calorimetric techniques with our methods for the generation of intense and stable metal cluster beams. We use a micromechanical calorimeter, which is based on microfabricated bimetallic cantilevers. The calorimeter allows us to measure the released heat during the deposition of a Sn_N cluster size distribution onto the solid surface of the sensor. The cantilever technique has the advantage of a very fast response time (1–5 ms) in combination with a very high heat sensitivity (10–100 pJ for a sensor area of 10^{-4} cm²), which is necessary for the thermal investigation of the very low cluster concentration in molecular beam experiments. The deposition process includes the condensation of isolated Sn_N clusters in the molecular beam (b) on the solid surface and results in the formation of bulk tin (s), which can be described by



wherein $q(b \rightarrow s)$ is the calorimetrically measured released heat per atom. This value will allow us to determine formation enthalpies of isolated clusters, if we correct the released heat taking the nonequilibrium situation of the cluster deposition process into account.

EXPERIMENTAL SETUP AND TIME-OF-FLIGHT ANALYSIS OF THE MOLECULAR BEAM

We have built up a high-vacuum molecular beam apparatus, which allows the generation of intense and stable metal and semiconductor cluster beams, in combination with a micromechanical calorimeter. This is schematically shown in Fig. 1. The molecular beam apparatus consists of a pulsed supersonic laser vaporization cluster source, which is described in detail elsewhere.⁶ The nozzle temperature of the cluster source is kept constant at 298 K in all the experiments. The size distribution of the investigated Sn_N clusters is probed by time-of-flight mass spectrometry. Photoionization of the neutral clusters is done with a Xe flash lamp and the investigation of the cluster cations, which are also generated in the cluster source, has been used to measure the Sn_N cluster size distribution in the pulsed molecular beam.

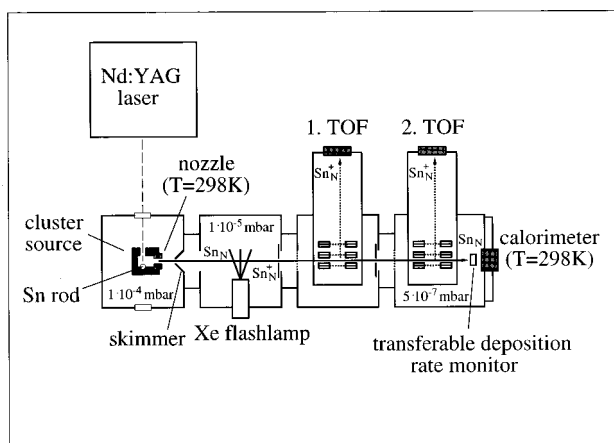


FIG. 1. Experimental setup of the molecular beam apparatus, which consists of a pulsed laser vaporization cluster source in combination with a micro-mechanical calorimeter.⁶ The apparatus is equipped with a Xe flash lamp for photoionization mass spectrometric investigations. Two time-of-flight mass spectrometers (1. and 2. TOF) enable us to determine the cluster velocities. The transferable quartz microbalance in front of the calorimeter allows a measurement of the deposition rate.

Figure 2 shows a time-of-flight mass spectrum of ionized neutral Sn_N clusters (b) and a mass spectrum of the cluster cations Sn_N^+ (a) recorded at the same source conditions. The photoionized neutral cluster size distribution and the one of the cluster cations can be characterized by the mean cluster size $\langle N \rangle$ of the mass spectrum. The mean cluster sizes agree within 10% for the cationic and the neutral clusters. This indicates that the distribution of the cluster cations is a measure for the neutral cluster size distribution in the molecular beam. This enables us to probe the molecular beam with a high repetition rate, i.e., a quasicontinuous time-of-flight mode, in order to determine the average cluster size distribution of the total cluster pulse. This procedure is necessary because the cluster size distribution varies over the total cluster pulse. The measurement of the average cluster size dis-

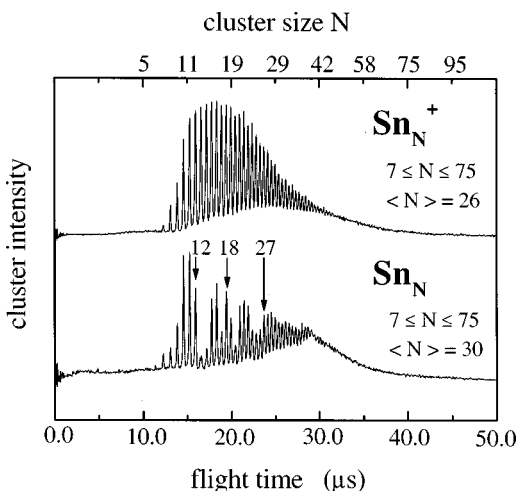


FIG. 2. Time-of-flight mass spectra of neutral Sn_N clusters ionized with a Xe flash lamp (b) in comparison with the cluster size distribution of the Sn_N^+ cations (a). Taking the intensities of the clusters I_N in each mass spectrum into account one can determine the mean cluster sizes to $\langle N \rangle = \sum N I_N / \sum I_N$ which agree within $\approx 10\%$ for the neutral and cationic clusters.

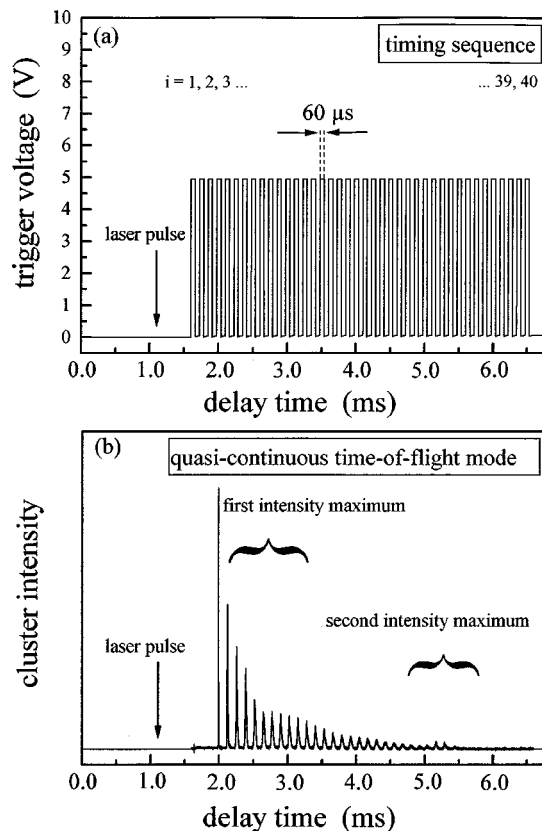


FIG. 3. (a) Timing sequence for the quasicontinuous time-of-flight mode: The delay time is the difference between the opening of the He valve and the acceleration of the cluster ions in the time-of-flight mass spectrometer. The 40 trigger pulses are generated at a repetition rate of 8 kHz. Each of the peaks shown in (b) represents a total time-of-flight mass spectrum of Sn_N^+ cluster cations, which is comparable to the one shown in Fig. 2(a). The peak height is a measure for the time-dependent integral intensity of cluster cations. Obviously two intensity maxima of cations are present in the cluster pulse.

tribution is done by recording time-of-flight mass spectra of the cluster cations generated in the cluster source at a fixed position of the molecular beam with a repetition rate of several kHz. The timing sequence with the corresponding measurement of 40 time-of-flight mass spectra at a repetition rate of 8 kHz is shown in Fig. 3. The size distribution of the Sn_N clusters deposited on the micromechanical calorimeter is obtained by averaging the 40 mass spectra measured over the total cluster pulse. This is shown in Fig. 4(a). The molecular beam contains Sn_N clusters with $N=6-600$ atoms, with a mean cluster size of $\langle N \rangle = \sum N I_N / \sum I_N = 142$ atoms, taking the cluster intensities I_N in the average mass spectrum into account.

Additionally a measurement of the velocities of the Sn_N clusters is necessary, because the calorimetrically measured released heat during the cluster deposition contains a contribution coming from the initial kinetic energy of the isolated clusters in the molecular beam. Therefore, we have set up two time-of-flight mass spectrometers, which are spatially separated at two fixed positions along the molecular beam (see Fig. 1). Recording time-of-flight mass spectra of cluster cations at these two fixed positions of the molecular beam with a repetition rate of again several kHz allows us to mea-

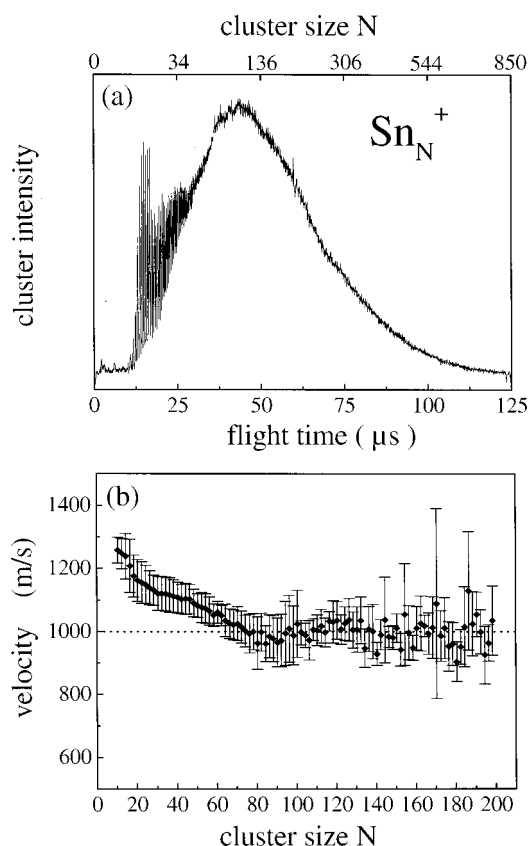


FIG. 4. (a) An average time-of-flight mass spectrum of the cations coming from the cluster source obtained from the 40 mass spectra shown in Fig. 3(b). The cluster pulse contains Sn clusters between $N=6$ and 600 atoms. The mean size is $\langle N \rangle = 142$ atoms per cluster. (b) Cluster velocities v_N obtained from time-of-flight measurements at two spatially separated positions of the molecular beam. For larger clusters ($N > 200$) a velocity of 1000 m/s can be used for the evaluation of the clusters' kinetic energy. Taking the error in the determination of the cluster velocities of about 70 m/s into account, one obtains a mean kinetic energy per atom of $e_{\text{kin}} = (0.62 \pm 0.09)$ eV.

sure the time-dependent intensity of each cluster size, which gives us the possibility to determine the cluster velocities v_N . The velocities of Sn_N clusters with up to $N=200$ atoms are shown in Fig. 4(b). For cluster sizes larger than $N=100$ we found velocities of 1000 m/s, which are constant within the error bars of about 70 m/s. Therefore, a cluster velocity of 1000 m/s can be used for the evaluation of the experimental results for Sn clusters with more than 200 atoms. The kinetic energy $E_{\text{kin}} = \frac{1}{2} m \sum_N N Z_N v_N^2$, which is transferred onto the micromechanical calorimeter during the deposition of the Sn_N cluster size distribution, depends on the mass m of the Sn atom, the cluster velocities v_N and the abundances Z_N of the clusters in the gas pulse. With the total number of deposited atoms $Z_a = \sum_N N Z_N$ per sensor area the kinetic energy per deposited atom is given by $e_{\text{kin}} = \frac{1}{2} m \sum_N N Z_N v_N^2 / \sum_N N Z_N$. Taking the cluster intensities $I_N \sim Z_N$ in the average mass spectrum into account, one obtains a mean kinetic energy per atom of $e_{\text{kin}} = (0.62 \pm 0.09)$ eV.

CONDENSATION OF ISOLATED Sn_N CLUSTERS ON A SOLID SUBSTRATE

We have achieved reproducible conditions for the deposition heat measurements in the high-vacuum apparatus with

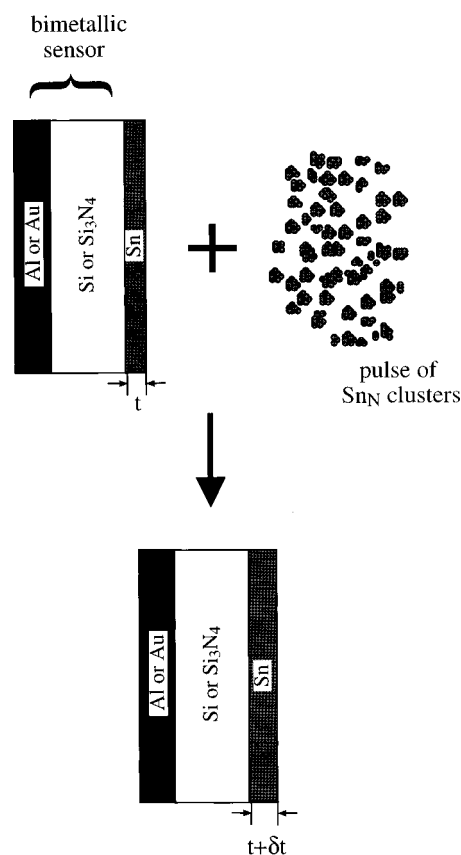


FIG. 5. Deposition of gas-phase Sn clusters: The thickness t of the bulk Sn layer on the bimetallic sensor is increased by δt with every deposited cluster pulse.

a typical He background pressure of about 5×10^{-7} mbar (the partial pressure of O_2 is below 10^{-7} mbar) at neutral cluster deposition rates of a few monolayers per minute determined at a distance of about one meter between the cluster source and the deposition rate monitor. The deposition of a Sn_N cluster size distribution on the micromechanical sensor increases the thickness t of the bulk Sn layer on the solid sensor surface with every deposited cluster pulse by δt , which is illustrated in Fig. 5. For the quantitative examination of the released heat during the formation of the bulk Sn films from the deposition of the isolated Sn_N clusters it is necessary to know the specific density of the Sn film, because the determination of the cluster film thickness and therefore of the absolute number of deposited clusters or cluster atoms with a quartz microbalance requires the density of the deposited cluster layer. We have determined the density of the Sn film ρ_{film} , by two independent thickness measurements. The thickness of the Sn cluster film is either measured with a quartz microbalance (t_{QM}) at a given density ρ and with an *ex situ* atomic force microscope (t_{AFM}).⁷ The density of the Sn cluster film is then given by the following relation $\rho_{\text{film}} = (t_{\text{QM}}/t_{\text{AFM}})\rho$. From the line scan in the AFM image in Fig. 6 one obtains the density of the Sn cluster film to 7200 kg/m^3 , which is close to the value of bulk tin at 298 K.⁸ This has been also confirmed by *ex-situ* x-ray diffraction, which demonstrates the formation of polycrystalline β -tin from the deposition of the isolated Sn_N clusters at room tem-

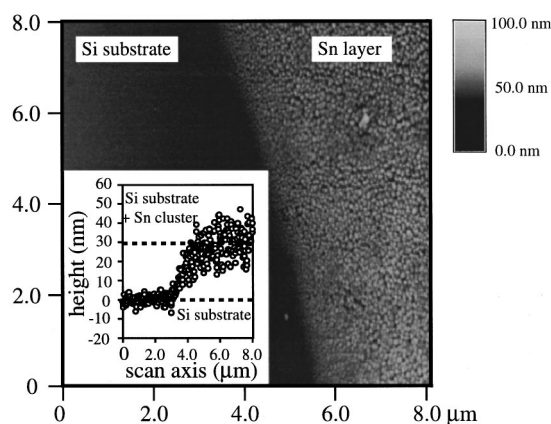


FIG. 6. Noncontact atomic force microscope (AFM) image⁷ of deposited Sn clusters on a Si substrate at 298 K. The deposition time was 180 min. The deposition rate of 1.6 \AA per minute has been measured with a quartz microbalance (QM) taking the formation of solid Sn films with a specific density of 7280 kg/m^3 into account. This results in a total film thickness of $t_{\text{QM}} = 28.8 \text{ nm}$. From the line scan in the AFM image one determines the film thickness to $t_{\text{AFM}} = (29.7 \pm 7.6) \text{ nm}$. This indicates that the density of the Sn cluster film is close to the value of bulk tin at 298 K. Therefore the bulk value has been used for the evaluation of the deposition rate.⁸ We have investigated the topography of the Sn films from the cluster deposition either in the contact and noncontact mode. The Sn islands with diameters between 30 and 130 nm visible in the topography have also been found at shorter deposition times and they seem to be typical for the growth of the deposited Sn clusters on the Si substrate.

perature (298 K). Another important point for the quantitative investigation of the heat measurements is the sticking behavior of the Sn_N clusters on the Sn film. We have not measured the sticking coefficient separately. However, data on atom⁵ and cluster⁹ sticking coefficient measurements indicate that one can assume a sticking probability equal to unity for substrates at room temperature. This assumption has been used in the evaluation of all the experimental data shown in this work.

MICROMECHANICAL CALORIMETER

The measurement of the released heat Q during the deposition of neutral Sn clusters is done with a two-component cantilever. The released heat ($Q < 0$) as a consequence of an exothermic cluster deposition process increases the cantilever's temperature ($\Delta T > 0$), which leads to a bending of the sensor towards the layer with the smaller expansion coefficient. The bending is measured from the deflection of a reflected laser beam on a position sensitive detector, which is schematically shown in Fig. 7. However, the total cantilever bending is also influenced by a transferred momentum P from the clusters' initial velocity. Therefore the measured voltage signal from the deflection of the laser beam on the position sensitive detector depends on the orientation of the cantilever relative to the cluster beam axis. This voltage signal U_{A-B} is proportional to the bending at the free end of the cantilever $\Theta_l = (dz/dx)_{x=l}$. The four different possibilities for the sensor orientation are shown in Fig. 8. For the configuration in Fig. 8(a) the total time-dependent cantilever bending $\Theta_l(t)$ is given by

$$\Theta_l(t) = \Theta_l^Q(t) - \Theta_l^P(t), \quad (2)$$

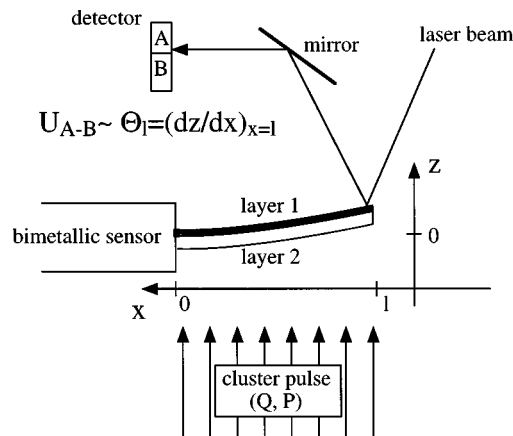


FIG. 7. Schematic description of the calorimeter, which is based on the bending measurement of a bimetallic cantilever. Layer 1 of the sensor corresponds to the material with the larger expansion coefficient (Al or Au) and layer 2 is the Si or Si_3N_4 body of the cantilever. The measured signal of the position sensitive detector U_{A-B} is proportional to the bending Θ_l at the free end of the sensor. The typical length l of the sensor is $500 \text{ }\mu\text{m}$ and the total sensor thickness is about $1 \text{ }\mu\text{m}$.

with the contributions Θ_l^Q and Θ_l^P from the released heat Q and the transferred momentum P , respectively. For a rectangular cantilever of length l and width w , which consists of two layers with thickness t_1 and t_2 , the heat and momentum contributions to the total bending Θ_l are described by the following formulas^{10,11}

$$\Theta_l^Q(t) = - \frac{2(\alpha_1 - \alpha_2)(t_1 + t_2)l^2}{t_2^2(t_1\lambda_1 + t_2\lambda_2)wK} \dot{Q}, \quad (3)$$

$$\Theta_l^P(t) = \frac{2(t_1E_1 + t_2E_2)l^2}{t_2^3t_1E_1E_2wK} \dot{P}, \quad (4)$$

$$K = 4 + 6\frac{t_1}{t_2} + 4\left(\frac{t_1}{t_2}\right)^2 + \frac{E_1}{E_2}\left(\frac{t_1}{t_2}\right)^3 + \frac{t_2E_2}{t_1E_1}, \quad (5)$$

wherein $\alpha_{1,2}$ are the thermal expansion coefficients, $\lambda_{1,2}$ the thermal conductivities, and $E_{1,2}$ the Young moduli of the two

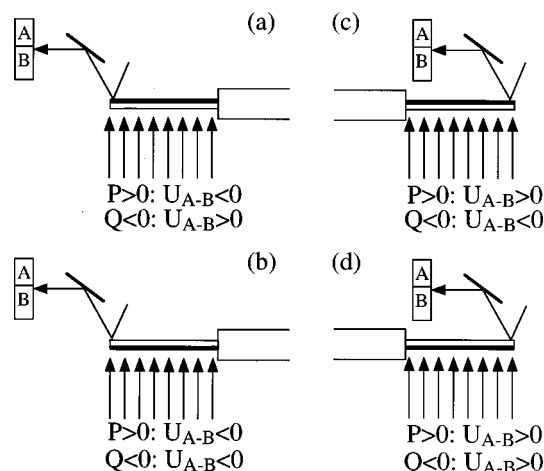


FIG. 8. The four different possible orientations of the bimetallic cantilever relative to the incoming cluster beam. The orientations in (b) and (d) represent a measurement with additive contributions from the released heat ($Q < 0$) and the transferred momentum ($P > 0$).

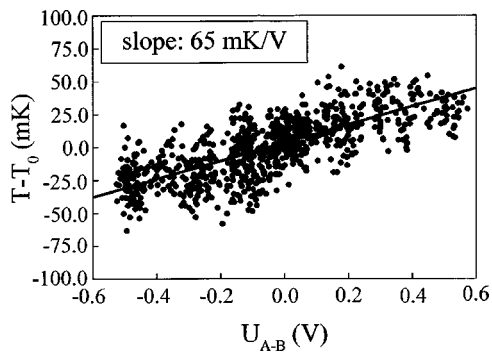


FIG. 9. Calibration of the apparatus constant c_{app} . The apparatus constant is determined from the slope 0.065 K/V of the temperature dependent position sensitive detector signal to $c_{app} = 9.56 \times 10^{-5} \text{ V}^{-1}$.

layers. A time-dependent measurement of the cantilever bending allows a determination of the released heat during the cluster deposition, if the contribution from the clusters' momentum transfer is known. However, the contribution from the clusters' momentum transfer is already determined from the measured cluster velocities v_N . The total transferred momentum by the cluster size distribution is given by $P = m \sum_N N Z_N v_N$. Taking the total number of deposited atoms on the cantilever area Z_a into account, one can determine the mean transferred momentum per deposited atom to $p = m \sum_N N Z_N v_N / \sum_N N Z_N$. With the cluster intensities $I_N \sim Z_N$ of the average mass spectrum one obtains the mean transferred momentum per deposited atom to $p = (1.99 \pm 0.14) \times 10^{-22} \text{ Ns}$. This allows us to calculate the total momentum transfer P on the cantilever, if the deposition rate or the deposited number of atoms Z_a on the cantilever area per pulse is known. The deposition rate measurement is done in front of the micromechanical calorimeter with a transferable quartz thickness monitor as indicated in Fig. 1. Typical deposition rates per cluster pulse are in the range of 10^{12} – 10^{13} atoms per cm^2 . This corresponds to a transferred momentum on the sensor of 10^{-13} – 10^{-14} Ns for a cantilever area of 10^{-4} cm^2 .

CALIBRATION OF THE CALORIMETER

In order to determine the total released heat Q from the measured voltage signal U_{A-B} of the position sensitive detector, one has to calibrate the apparatus constant c_{app} of the calorimeter. This is done with a resistance heater, in which the bimetallic cantilever is mounted. Due to the small response time of the cantilever, the heat exchange between the heater and the sensor is very fast. This allows one to determine the shift of the cantilever temperature from the measured temperature of the heating cell. The temperature dependent bending $\Theta_l(t)$ of the bimetallic cantilever is given by^{10,11}

$$\Theta_l(t) = \frac{6(\alpha_1 - \alpha_2)(t_1 + t_2)l}{t_2^2 K} (T - T_0) = c_{app} U_{A-B}, \quad (6)$$

wherein T_0 is a reference temperature. The calibration measurement for the bimetallic cantilever used for the bending measurements in Fig. 10 is shown in Fig. 9. From the slope 0.065 K/V of the temperature dependent U_{A-B} signal one

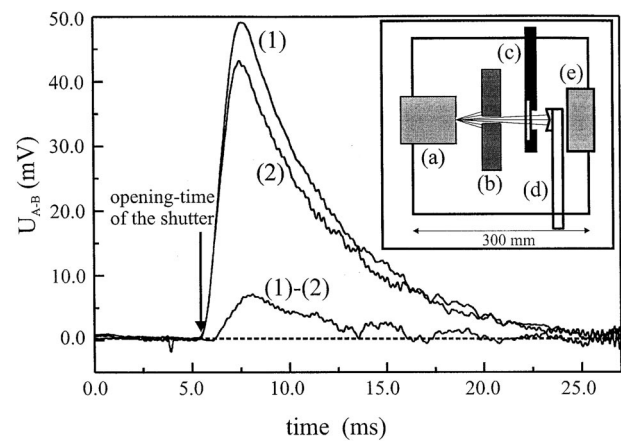


FIG. 10. Measurement of the formation enthalpy of Sn atoms coming from a pulsed Knudsen cell. The inset shows the particular setup for the experiment: (a) Knudsen cell, (b) mechanical shutter,¹² (c) transferable BaF_2 window,^{5,14} (d) transferable quartz microbalance, (e) micromechanical calorimeter. The cantilever bending has been measured with the orientation shown in Fig. 8(a). The bending curves of the bimetallic cantilever¹³ correspond to the heat of radiation with (1) and without (2) the contribution from the atomic beam. The third curve, i.e., the difference $(1) - (2)$, is the sensor bending which is only due to the contribution from the atomic Sn beam. The deposition rate of 8.8×10^7 atoms at an oven temperature of 1560 K results in a released heat of 35.2 pJ for the Sn atom deposition. The measured bending curve for the heat of radiation (2) allows one additionally to determine the thermal response time of the calorimeter. An exponential fit to the measured curve results in a response time of $\tau_Q(\text{exp.}) = 5.0 \text{ ms}$. This value can be compared to the theoretically expected response time of a bimetallic cantilever.¹⁰ It could be estimated from the mechanical and thermal properties of the sensor to $\tau_Q = 6.2 \text{ ms}$, which is in good agreement with the experimental value.

determines the apparatus constant to $c_{app} = 9.56 \times 10^{-5} \text{ V}^{-1}$. In order to prove the validity of the calorimeter calibration we have applied the bimetallic cantilever to determine the formation enthalpies of Sn atoms coming from a pulsed Knudsen cell. The setup for this particular experiment is shown in the inset of Fig. 10. With a mechanical shutter¹² pulses of Sn atoms with a typical width of a few ms are transmitted onto the micromechanical calorimeter. The deposition of these Sn atoms leads to a deflection of the bimetallic cantilever.¹³ However, one has to take into account that also heat radiation from the oven is transmitted to the calorimeter when the shutter opens. Therefore one has to measure the radiation contribution to the sensor bending in an additional experiment, where a BaF_2 window^{5,14} is moved into the atomic beam. The time-dependent sensor bending with (1) and without (2) the heat contribution from the atomic beam is shown in Fig. 10 for a deposition rate of $Z_a = 8.8 \times 10^7$ atoms per pulse. These measurements are averaged over 500 pulses. The effective sensor bending due to the deposition of Sn atoms $(1) - (2)$ is also a consequence of a transferred momentum p per atom¹⁵ in combination with the released heat q . For the measurement in Fig. 10 at an oven temperature of 1560 K one determines a released heat of 2.50 eV per atom. Averaging all the measurements we found a released heat of $q = (3.45 \pm 1.20) \text{ eV}$. In order to determine the formation enthalpy, which refers to the substrate temperature of 298 K, one has to take the enhanced kinetic energy of the Sn atoms in the atomic beam into account.¹⁵ This results follow-

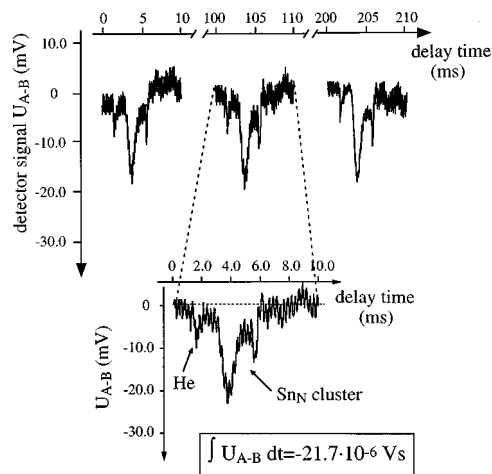


FIG. 11. Typical bending measurements of a Au coated Si_3N_4 cantilever¹³ during the pulsed cluster deposition [see sensor orientation in Fig. 8(a)]. The repetition rate of the cluster machine is 10 Hz. The first peak of the bending curve is due to the transferred momentum of scattered He atoms coming from the cluster source. The height and shape of the second and third peak are a consequence of the time-dependent density of clusters in the gas pulse [see also Fig. 3(b)]. The appearance and shape of these peaks depend strongly on the operation conditions of the cluster source. The integration of the time-dependent sensor bending corresponds to a released heat of -27.6 pJ at a deposition rate of 1.8×10^8 atoms per sensor area. The deflection signal is modulated by the thermally excited resonance frequency of the cantilever (≈ 5500 Hz). This effect limits the heat resolution of the calorimeter.

ing the procedure described by Campbell *et al.*⁵ in a formation enthalpy of $\Delta h_{f,298}(\text{Sn}(g)) = (3.25 \pm 1.20)$ eV per atom. This value is 3% above the literature value of 3.12 eV.¹⁶ The large error in the measured formation enthalpy is a consequence of the strong radiation contribution of 87% to the total sensor bending.

However, the atomic beam experiment demonstrates the capability of our setup and allows the application of the micro-mechanical calorimeter to the investigation of the deposition process of Sn clusters from a pulsed molecular beam.

CALORIMETRIC HEATS FOR THE DEPOSITION OF Sn_N CLUSTERS

A series of three typical time-dependent bending measurements is shown in Fig. 11 during the Sn_N cluster deposition of $Z_a = 1.8 \times 10^8$ atoms per pulse on an Au/ Si_3N_4 composite cantilever.¹³ The curves are time-averaged over 300 cluster pulses. The inset shows a magnified bending measurement, in which three peaks can be identified. The first one is due only to momentum transfer from the He carrier gas. The second and third peak [see time-of-flight analysis of the cluster pulse in Fig. 3(b)] are a result of the cluster deposition, i.e., the released heat Q in combination with the transferred momentum P . The bending curve has been measured with the cantilever orientation shown in Fig. 8(a). This demonstrates that the measured signal from the position sensitive detector U_{A-B} resulting from the transferred momentum P is larger than that from the released heat Q . The integrated detector signal corresponds to a total bending of $\int \Theta_I(t) dt = -1.91 \times 10^{-9}$ s. The apparatus constant for this experiment has been determined to $c_{\text{app}} = 8.82 \times 10^{-5} \text{ V}^{-1}$. With

the total transferred momentum $P = Z_a p = 3.63 \times 10^{-14}$ Ns one calculates the released heat per cluster pulse to $Q = -27.6$ pJ. The measured calorimetric heat per deposited atom is $q = -0.94$ eV. Before we have started the heat measurements a Sn cluster layer of $t \approx 1$ nm has been deposited on the bimetallic cantilever. The heat experiments have been stopped before the Sn cluster layer reaches a thickness of $t \approx 5$ nm. Before and after a series of heat measurements the apparatus constant of the calorimeter was constant within 10%. We have also examined the dependence of the apparatus constant c_{app} on the heating rate. We found a constant value of c_{app} for heating rates between 0.001 and 0.1 K/s. This indicates that the calibration method is also applicable to the pulsed cluster experiment with a typical increase of the cantilever temperature of 1 K/s. In order to estimate the influence of the Sn cluster layer on the evaluation of the experimental data one can describe the three layer cantilever ($\text{Sn}/\text{Si}_3\text{N}_4/\text{Au}$) as a simple bimetallic cantilever with an effective Au layer thickness, because the Sn_N clusters are deposited opposite to the Au layer thereby reducing the bimetallic effect [see cantilever orientation in Fig. 8(a)]. In this model it has been assumed that the Sn layer does not influence the mechanical and thermal properties of the cantilever. The difference in the thermal expansion coefficients between the Au and Sn layer has also been neglected. Within this assumption the measured released heat will be increased by only 7% for the largest deposited Sn layer of 5 nm, which is still in the uncertainty of the calibration measurement. In order to confirm the value of the measured calorimetric heat, we have measured the released heats with different bimetallic cantilevers, consisting of various materials and in different orientations. For example, we have studied the bending of cantilevers, which consist of a fixed Si_3N_4 body (550 nm), in dependence of a variable gold layer thickness (50–110 nm), finding the same value of the released heat. The mean value of the measured calorimetric heat per atom is $q = -(1.07 \pm 0.19)$ eV. We have analyzed our measurements also with a nonunity sticking probability. A deviation from the assumed unity sticking behavior of 1% will increase the measured deposition heats by only 3%.

COMPLEMENTARY MEASUREMENTS

Figure 12 shows time-dependent bending measurements for a 700 nm Al coated 2200 nm thick Si body¹⁷ at two different orientations of the sensor relative to the cluster beam axis. The orientation for the measurement in Fig. 12(a) with the open circles is equal to that illustrated in Fig. 8(d), the measurement with the open squares corresponds to the orientation shown in Fig. 8(c). For this sensor the contribution from the released heat to the total time-dependent bending is larger than the one due to the transferred momentum. The two “complementary” measurements give us the possibility to determine Q and P without any external momentum measurement, because in one case the sensor orientation causes both effects to be additive [Fig. 12(a): open circles], whereas in the other case the contribution from the released heat is opposite to the momentum transfer [Fig. 12(a): open squares]. Subtracting and adding both measurements results

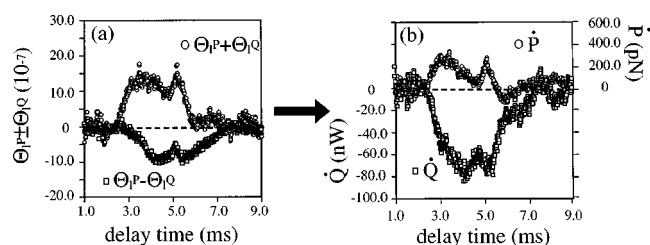
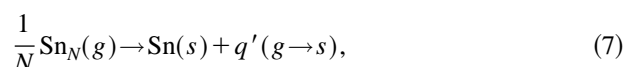


FIG. 12. (a) “Complementary” bending measurements with an Al coated Si cantilever¹⁷ in two different orientations with a deposition rate of $Z_a = 1.4 \times 10^9$ atoms per sensor area and cluster pulse. The curve with the open circles is the additive measurement [see sensor orientation in Fig. 8(d)], the curve with the open squares corresponds to an opposite contribution of heat and momentum [see sensor orientation in Fig. 8(c)]. The peak from the scattered He atoms is missing, since the sensor is less sensitive to the momentum contribution. (b) Pure heat (open circles) and momentum (open squares) behavior resulting from the “complementary” measurements in (a).

in the pure heat and momentum contributions shown in Fig. 12(b). From the integration of the time-dependent sensor bending one determines the released heat to $q = -(1.1 \pm 0.2)$ eV, which is in good agreement with the previous measurements. The transferred momentum is determined to $p = (2.8 \pm 1.0) \times 10^{-22}$ Ns per deposited atom. The large uncertainty of the value is a consequence of the small sensitivity of the cantilever to the momentum contribution. However, the value is still in reasonable agreement with the one determined from the time-of-flight analysis in combination with the assumed unity sticking behavior of the clusters on the solid surface. For this bimetallic cantilever the influence of the deposited Sn layer (5 nm) in the evaluation of the released heat is about 1%.

RELATING THE MEASURED CALORIMETRIC HEAT TO THE FORMATION ENTHALPY OF THE METAL CLUSTERS

The nonequilibrium situation of the cluster deposition process in the molecular beam experiments described here makes a correction of the calorimetrically measured heats $q(b \rightarrow s)$ necessary, in order to obtain formation energies or enthalpies for the isolated clusters, which are equivalent to a hypothetical situation, in which a vapor of Sn_N clusters (g) is in equilibrium with a solid Sn substrate (s). This situation can be described by



wherein $q'(g \rightarrow s)$ is the released heat per atom of the equilibrium process. First, and this is the major correction to the measured heat $q(b \rightarrow s)$, one has to take the enhanced kinetic energy of the isolated clusters into account, which the clusters gained during the supersonic expansion into vacuum. Since the kinetic energy of the isolated cluster is much larger than the one of a cluster in a hypothetical vapor in equilibrium with a solid substrate at a temperature of 298 K, one arrives at a corrected released heat per atom $\tilde{q} = q(b \rightarrow s) + 0.62$ eV by taking the heat contribution from the kinetic energy per atom e_{kin} into account. A correction due to the kinetic energy from the perpendicular velocity components

($v_{\perp} < 0.1$ m/s) of the isolated clusters is negligible. Since the cluster deposition in our experiments involves no pressure–volume work of compression against external constraint, the corrected calorimetric heat is directly related to an internal energy change and not an enthalpy change. The measured calorimetric heat per atom for a given pulse of Sn_N clusters is therefore just the internal energy difference between an initial state consisting of a solid Sn surface at 298 K and a pulse of gaseous Sn clusters coming from a supersonic cluster source with a nozzle also at a temperature of 298 K. This means that the corrected released heat \tilde{q} measures the formation energy of the isolated clusters. However, additionally one has to take the influence of the clusters’ internal degrees of freedom on the measured released heats into account, because the vibrations and rotations of the isolated clusters could be significantly cooled during the supersonic expansion. Since the exact rotational and vibrational temperatures T_r and T_v of the isolated clusters in the molecular beam are unknown, one can consider two extreme cases, in order to obtain a lower and upper limit for the formation energy: a total cooling of the cluster vibrations and rotations $T_v = T_r = 0$ K or vibrational and rotational temperatures, which are equal to the nozzle temperature (=substrate temperature T_s) $T_v = T_r = T_s$. Thus for large clusters ($N \gg 1$) one arrives for the formation energy per atom $\Delta u_{f,T_s} = q'$ at the following relation:

$$-\tilde{q} \leq \Delta u_{f,T_s} \leq -\tilde{q} + 3kT_s. \quad (8)$$

This value of the formation energy now allows a comparison with data obtained from experiments under equilibrium conditions. Formation enthalpies of the isolated clusters can be obtained taking the pressure volume work into account, which in the case of an assumed ideal behavior is only an additional term of kT_s per cluster to the formation energies. For the investigated cluster sizes ($N \gg 1$) formation enthalpies per atom are therefore in a good approximation equal to the corresponding formation energies $\Delta h_f = \Delta u_f$. The lower and upper limit of the formation enthalpy per atom for the investigated Sn cluster size distribution are therefore determined to $0.45 \text{ eV} < \Delta h_{f,298} < 0.53 \text{ eV}$.

DISCUSSION

Neglecting considerable changes in the chemical bonds between the atoms in the clusters compared to the bulk, the formation enthalpy per atom is, in a simple thermodynamic picture, a consequence of the free surface area A of the isolated clusters. Therefore, one can estimate the formation enthalpy of a cluster from its surface enthalpy. However, one problem in this approach is the unknown temperature dependent surface tension $\sigma(T)$, i.e., the entropic contribution to the surface enthalpy at a finite temperature. However, one can try to approximate the measured formation enthalpies per atom for a spherical cluster with N atoms at 298 K from the surface enthalpy at $T = 0$ K (Ref. 18) by the following formula

$$\Delta h_{f,0} = \frac{(A\sigma)_{T=0 \text{ K}}}{N} = 4\pi r_{\text{WS}}^2 \sigma_0 N^{-1/3}, \quad (9)$$

wherein r_{WS} is the Wigner–Seitz radius of bulk β -tin and σ_0 the surface tension of a flat tin surface at 0 K.¹⁹ In this formula also the curvature of the cluster surface has been neglected. Taking the average cluster size distribution into account [see mass spectrum in Fig. 4(a)], one calculates a mean surface enthalpy per atom of 0.36 eV. Considering the assumptions made, the value from the surface energy model is in a reasonable agreement with the experimental value of 0.45–0.53 eV, which indicates that the formation enthalpy of the investigated metal cluster size distribution is strongly dominated by the clusters' free surface area.

ACKNOWLEDGMENT

We acknowledge the strong support from Professor H.-J. Güntherodt. R.S. wishes to thank Professor J. A. Becker (University Hannover) for several discussions concerning the thermodynamics of the cluster deposition process and for providing us with the Knudsen cell. The work is supported by the Swiss National Science Foundation within the Research Equipment Program.

¹J. Drowart and P. Goldfinger, *Angew. Chem.* **79**, 589 (1967).

²K. A. Gingerich, A. Desideri, and D. L. Cocke, *J. Chem. Phys.* **62**, 731 (1975).

³W. A. de Heer, *Rev. Mod. Phys.* **65**, 611 (1993).

⁴C. E. Borroni-Bird, N. Al-Sarraf, S. Anderson, and D. A. King, *Chem. Phys. Lett.* **183**, 516 (1991); C. E. Borroni-Bird and D. A. King, *Rev. Sci. Instrum.* **62**, 2177 (1991).

⁵J. T. Stuckless, D. E. Starr, D. J. Bald, and C. T. Campbell, *J. Chem. Phys.* **107**, 5547 (1997). J. T. Stuckless, N. A. Frei, and C. T. Campbell, *Rev. Sci. Instrum.* **69**, 2427 (1998).

⁶T. Bachels and R. Schäfer, *Rev. Sci. Instrum.* **69**, 3794 (1998).

⁷The atomic force microscope measurements are performed with a Nano-

scope IIIa from Digital Instruments (Santa Barbara, California). The resonance frequency of the Si cantilever for the noncontact image was ≈ 300 kHz (Nanosensors, Dr. Olaf Wolter GmbH, IMO-Building, Im Amtmann 6, D-35578 Wetzlar-Blankenfeld, Germany).

⁸The density ρ of the thermodynamic stable Sn modification at 298 K is 7280 kg/m³: R. A. Robie, P. M. Bethke, and K. M. Beardsley, in *Handbook of Chemistry and Physics*, 72nd ed. edited by D. R. Lide (CRC, Boston, 1991), p. 4–156.

⁹V. Philipps, E. Vietzke, and K. Flaskamp, *Surf. Sci.* **178**, 806 (1986).

¹⁰J. R. Barnes, R. J. Stephenson, C. N. Woodburn, S. J. O'Shea, M. E. Welland, T. Rayment, J. K. Gimzewski, and Ch. Gerber, *Rev. Sci. Instrum.* **65**, 3793 (1994).

¹¹R. J. Roark and W. C. Young, *Formulas for Stress and Strain*, 5th ed. (McGraw-Hill, New York, 1975), pp. 113 and 576.

¹²JML Optical Industries, Rochester, New York: Model SES 16505.

¹³The dimensions and properties of the triangular Au coated Si₃N₄ cantilever are as follows: $t_1 = 50$ nm Au, $t_2 = 550$ nm Si₃N₄, $w = 35$ μ m, $l = 330$ μ m, $\alpha_1 = 14.2 \times 10^{-6}$ K⁻¹, $\alpha_2 = 3.2 \times 10^{-6}$ K⁻¹, $\lambda_1 = 317$ W(mK)⁻¹, $\lambda_2 = 19$ W(mK)⁻¹, $E_1 = 80$ GPa, $E_2 = 180$ GPa.

¹⁴The transmission of the BaF₂ window is 92%: *American Institute of Physics Handbook*, edited by D. E. Gray, Ed. III (McGraw-Hill, New York 1972), pp. 6–63.

¹⁵The mean transferred momentum of a Sn atom at an oven temperature T onto the calorimeter is $p = (2\pi mkT)^{1/2}$. The mean kinetic energy of the Sn atoms in the atomic beam is equal to $e_{\text{kin}} = 2kT$ [see for example G. Comsa and R. David, *Surf. Sci. Rep.* **5**, 145 (1985)].

¹⁶D. D. Wagman, W. H. Evans, V. B. Parker, R. H. Schumm, S. M. Bailey, J. Halow, K. L. Chumey, and R. L. Nuttall, in *Handbook of Chemistry and Physics*, edited by D. R. Lide, 72nd ed. (CRC, Boston 1991), pp. 5–57.

¹⁷The dimensions and properties of the rectangular Al coated Si cantilever are as follows: $t_1 = 700$ nm Al, $t_2 = 2200$ nm Si, $w = 54$ μ m, $l = 444$ μ m, $\alpha_1 = 23.2 \times 10^{-6}$ K⁻¹, $\alpha_2 = 4.7 \times 10^{-6}$ K⁻¹, $\lambda_1 = 237$ W(mK)⁻¹, $\lambda_2 = 124$ W(mK)⁻¹, $E_1 = 80$ GPa, $E_2 = 169$ GPa.

¹⁸A. R. Miedema and J. W. F. Dorleijn, *Philos. Mag. B* **43**, 251 (1981).

¹⁹W. R. Tyson and W. A. Miller, *Surf. Sci.* **62**, 267 (1977); J. P. Perdew, Y. Wang, and E. Engel, *Phys. Rev. Lett.* **66**, 508 (1991).